Supporting Information

In vivo imaging of senescent vascular cells in atherosclerotic mice using a *β*-galactosidase-activatable nanoprobe

Ji-An Chen[a‡], Wei Guo[a‡], Zhijun Wang[a], Nannan Sun[a], Hongming Pan[a], Jiahui Tan[a], Zhirong Ouyang [a], Wei Fu[a], Yonghui Wang[a], Wei Hu[a], Xianfeng Gu[a]**

[a] *School of Pharmacy & Minhang Hospital, Fudan University, Shanghai 201301, China*

[*]Correspondence: xfgu@fudan.edu.cn ; 18918169120@163.com

[‡] Contribution equally

Table of Contents

Experimental Procedures

General Information: All commercially available solvents and chemicals were used without further purification unless special stated. ^{1}H NMR and ^{13}C spectra were recorded on a Bruker AV-400 and AV 600 MHz instruments with chemical shifts reported in ppm. Deuterated chloroform and Deuterated DMSO were used as the solvent, TMS as the internal standard. Mass spectra were measured on an HP 1100 LC-MS spectrometer.

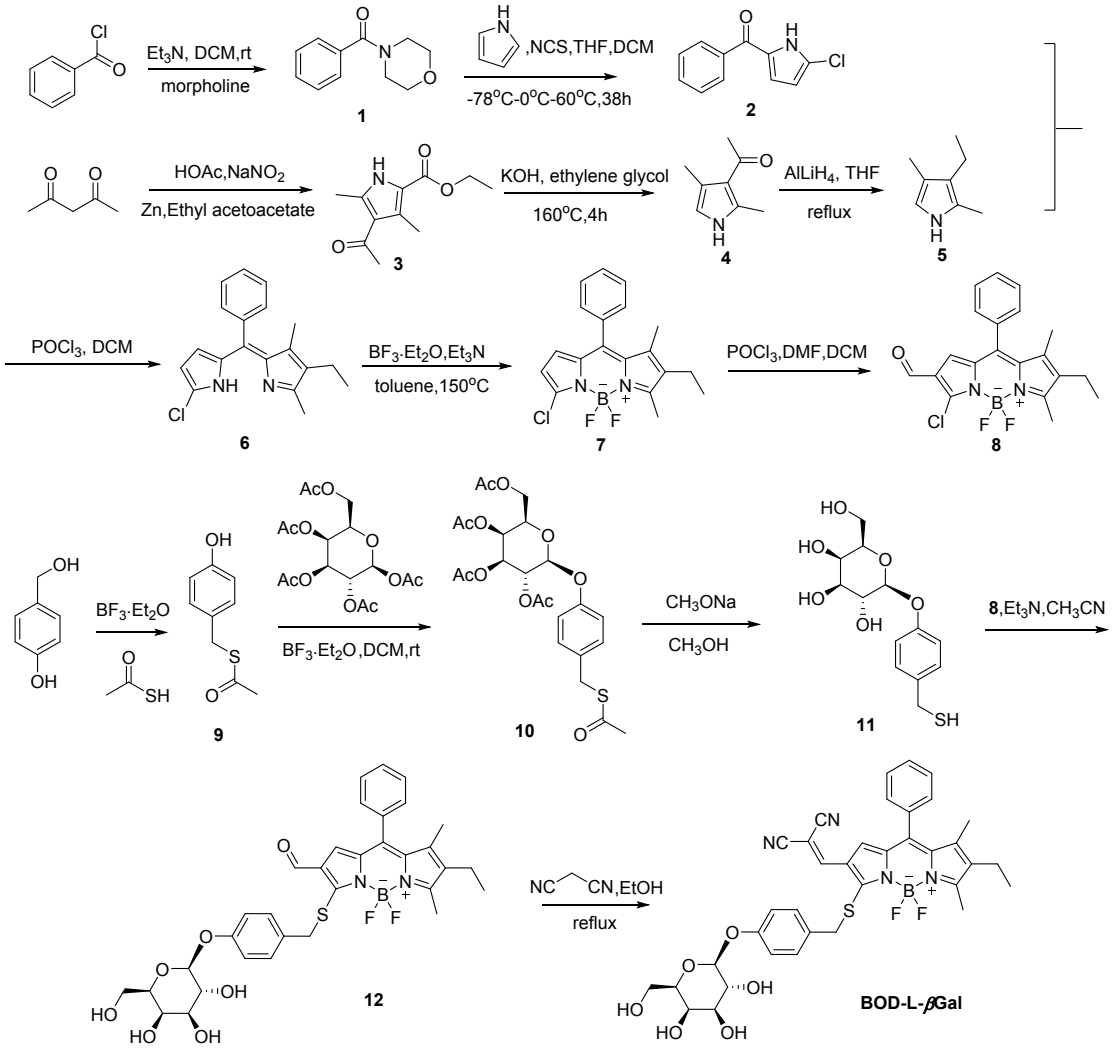

Scheme S1 Synthetic route of **BOD-L-*β*Gal**

Synthesis of compound 1

Benzoyl chloride 23.11 mL (28.2 g, 0.2 mol) was added to a solution of trimethylamine (41.72 mL, 30.3g, 0.3mol) and morpholine (23.11 mL, 28.2 g 0.2 mol) in DCM (300 mL) at room temperature. The mixture was stirred for 2 h and then diluted with DCM (200 mL). The solid was removed by filtration and the filtrate was washed by brine, dried over anhydrous sodium sulfate. The organic layer was evaporated in vacuum and crystallized to afford **1** (35.16 g, 91%). ^{1}H NMR (400MHz, $CDCl_3$), δ 7.89 (d, 2H), 7.58 (t, 1H), 7.48 (t, 2H), 3.72 (t, 4H), 3.49 (t, 4H). ESI-MS calculated for $C_{11}H_{14}NO_2^+$ $[M+H]^+$: 192.1, found: 192.1.

Synthesis of compound 2[1]

Sulfuryl chloride (5.32 g, 40 mmol) dissolved in THF (100 mL) was added in a dropwise manner to a stirred solution of pyrrole (2.68 g, 40 mmol) in anhydrous THF (160 mL) under nitrogen at -78 °C. The solution was stirred at -78 °C for 30 min, and then placed in -20 °C for 14 h. The cooled solution was then brought to 0 °C and stirred for 6 h. Mixed *N*-morpholinoylamide (11.4 g, 60 mmol) and $POCl_3$ (19.92 g, 130 mmol) at 0 °C and stired the mixture at room temperate for 6 h to form the acylating agent. The acylating agent was diluted with 40 mL DCM and added dropwise in to the solution over 30 min. The resulting solution was stirred at room temperature for 14 h. An aqueous solution of NaOAc (140 mmol in 400 mL H_2O) was added in the solution and the mixture was refluxed for 30min. the mixture was extracted with diethyl ether, washed with saturated $NaHCO_3$ (until basic) and brine (until neutral). The organic layer was dried over anhydrous sodium sulfate, filtered and evaporated in vacuum. The residue was purified by silica gel column (hexane/ethyl acetate; 50:1) to give **2** (2.02 g, 24%). ^{1}H NMR (400MHz, $CDCl_3$), δ 9.98 (s, 1H), 7.87 (d, J =7.6 Hz, 2H), 7.58 (t, J =7.3 Hz, 1H), 7.49 (t, J =7.3 Hz, 2H), 6.82 (s, 1H), 6.20 (s, 1H). ESI-MS calculated for $C_{11}H_9ClNO^+$ $[M+H]^+$: 206.0, found: 206.1.

Synthesis of compound 3

An aqueous solution of $NaNO_2$ (15 g, 0.216 mol) was added in the solution of acetoacetate (26 g, 0.2 mol) in AcOH (52ml), stirred overnight. To the solution was added 2,4-pentane-dione (20g, 0.2 mol), followed by Zn dust (28.1 g, 0.43 mol) under the ice bath. After heated to 60 °C for 1 h, the reaction mixture was filtered, extracted with DCM, dried over anhydrous sodium and evaporated in vacuum. The

residue was washed with cold EtOH to gain **3** (35.4 g, 85%). ^{1}H NMR (400MHz, $CDCl_3$), δ 9.05 (s, 1H), 4.37-4.31 (q, *J* = 7.1 Hz, 2H), 2.59 (s, 3H), 2.52 (s, 3H), 2.45 (s, 3H), 1.38 (t, *J* = 7.1 Hz, 3H). ESI-MS calculated for $C_{11}H_{16}NO_3^+$ $[M+H]^+$: 210.1, found: 210.1.

Synthesis of compound 4[2]

A mixture of **3** (35.4 g 0.17 mol) and KOH (14.2 g, 0.25 mol) in ethtlene glycol (100 mL) was heated at 160 °C for 4 h. After cooling to room temperature, the solution was extracted with DCM, and the extract was washed by brine, dried and evaporated to afford **4** (20.9g, 90%). ^{1}H NMR (400MHz, DMSO-d_6), δ 10.91 (s, 1H), 6.39 (s, 1H) 2.38 (s, 3H), 2.29 (s, 3H) 2.15 (s, 3H). ESI-MS calculated for $C_8H_{12}NO^+$ $[M+H]^+$: 138.1, found: 138.1.

Synthesis of compound 5[2]

To 200 mL of dry THF was added **4** (20.9g, 0.15 mol) and 150 mL of 1M $LiAlH_4$ in an ice bath. The solution was refluxed for 4.5 h and brought to room temperature, then, the excess $LiAlH_4$ was quenched with sodium sulfate decahydrate. The solid was removed by filtration and the filtrate was washed by brine, dried over Na_2SO_4 and evaporated in vacuum to afford crude product **5** ready for next step. ESI-MS calculated for $C_8H_{14}N^+$ $[M+H]^+$: 124.1, found: 124.3.

Synthesis of compound 6

A mixture of **2** (2.02 g, 9.8 mmol) and $POCl_3$ (2.09 mL, 3.45 g, 22.54 mmol) in 10 mL dry DCM was stirred for 1 h at room temperature under argon protection. To this solution was added **5** (3.69 g, 30 mmol) in mL DCM, and the mixture was further stirred at room temperature for 48 h. Then, the solution was slowly poured into saturated $NaHCO_3$ under ice-cold conditions, washed with brine, dried over Na_2SO_4 and evaporated in vacuum to afford crude product **6** ready for next step. ESI-MS calculated for $C_{19}H_{20}ClN_2^+$ $[M+H]^+$: 311.1, found: 311.2.

Synthesis of compound 7

To mL of toluene was added **6** (2.42 g, 7.8 mmol) and Et_3N (3.25 mL, 2.36 g, 23.4 mmol) in an ice bath. After stirring for 1 h at room temperature, $BF_3{\cdot}OEt_2$ (3.94 mL, 4.43 g, 31.2 mmol) was added and the reaction was stirred at 100 °C for 6 h. When the reaction was cooled to room temperature, the reaction

mixture was diluted with DCM and washed with saturated $NaHCO_3$ solution and brine, dried over Na_2SO_4 and evaporated. The residue was purified by silica gel column (hexane: DCM: ethyl actate = 80: 20: 10) to give **7** (2.54 g, 91%). ^{1}H NMR (400MHz, $CDCl_3$), δ 7.51 -7.44 (m, 1H), 7.31 (m, 2H), 6.24 (d, J = 3.8 Hz, 1H), 6.20 (d, J = 3.8 Hz, 1H), 2.63 (s, 3H), 2.35 (q, J = 7.6 Hz, 2H), 1.43 (s, 3H), 1.02 (t, J = 7.6 Hz, 3H). ESI-MS calculated for $C_{19}H_{18}BClF_2N_2Na^+$ $[M+Na]^+$: 381.1, found: 381.2.

Synthesis of compound 8

To 15 mL of DMF was added $POCl_3$ (15 mL) in an ice bath. After warmed to room temperature, it was stirred for additional 30 min. To this solution was added **7** (1.5 g, 4.1 mmol) in 50 mL DCM, and the mixture was further stirred at room temperature for 24 h. Subsequently, the mixture was slowly poured into saturated $NaHCO_3$ under ice-cold conditions, extracted with DCM, washed with brine, dried over Na_2SO_4 and evaporated. The residue was further purified using silica gel column (hexane: DCM: ethyl actate = 350: 50: 10) to give **8** (586mg, 37%). ^{1}H NMR (400MHz, $CDCl_3$), δ 1.08 (t, J = 7.6 Hz, 3H), 1.49 (s, 3H), 2.38 (q, J = 7.6 Hz, 2H), 2.69 (s, 3H), 6.64 (s, 1H), 7.28 (m, 2H), 7.52 (m, 3H), 9.85 (s, 1H). ESI-MS calculated for $C_{20}H_{19}BClF_2N_2O^+$ $[M+H]^+$: 387.1, found: 387.3.

Synthesis of compound 9[3]

To (4-hydrooxyphenyl)methanol (12 g, 96 mmol) suspended in thioacetic acid (72 mL) was added $BF_3{\cdot}OEt_2$ (1.8 mL, 13.2 mmol). After stirring for 3 h at room temperature, the solution was diluted with EtOAc (80 mL), washed with saturated $NaHCO_3$ and brine, dried over Na_2SO_4, filtered and evaporated. The crude product was purified by silica gel column (hexane: ethyl actate = 20: 1) to give **9** (14 g, 80%). ^{1}H NMR (400MHz, $CDCl_3$), δ 2.27 (s, 3H), 3.99 (s, 2H), 5.66 (s, 1H), 6.98 (d, J = 8.1 Hz, 2H), 7.07 (d, J = 8.1 Hz, 2H). ESI-MS calculated for $C_9H_{10}NaO_2S^+$ $[M+Na]^+$: 205.0, found: 205.1.

Synthesis of compound 10[3]

To 300 mL freshly distilled DCM was added *β-D*-galactose peracetate (12.5 g, 32 mmol), **9** (11.7 g, 64 mmol) and $BF_3{\cdot}OEt_2$ (20 mL, 128 mmol). After stirring for 36 h at room temperature, the solution was diluted with DCM, washed with saturated $NaHCO_3$ and brine, dried over Na_2SO_4 and evaporated. The residue was purified by silica gel column (hexane: ethyl actate = 4: 1) to afford **10** (7.4 g, 45%). ^{1}H NMR

(600 MHz, DMSO-d_6) δ 7.25 (d, J = 8.6 Hz, 2H), 6.92 (d, J = 8.6 Hz, 2H), 5.42 (d, J = 7.9 Hz, 1H), 5.33 (d, J = 3.5 Hz, 1H), 5.27 (dd, J = 10.4, 3.5 Hz, 1H), 5.19 (dd, J = 10.3, 7.9 Hz, 1H), 4.41 (t, J = 6.4 Hz, 1H), 4.09 (dd, J = 6.4, 3.8 Hz, 2H), 4.07 (s, 2H), 2.34 (s, 3H), 2.14 (s, 3H), 2.03 (s, 3H), 2.00 (s, 3H), 1.94 (s, 3H). ^{13}C NMR (151 MHz, DMSO-d_6) δ 194.83, 169.97, 169.83, 169.55, 169.21, 155.55, 132.29, 130.01, 116.47, 97.78, 70.30, 70.13, 68.33, 67.20, 61.28, 39.52, 31.83, 30.27, 20.47, 20.43, 20.39, 20.34.ESI-MS calculated for $C_{23}H_{28}NaO_{11}S^+$ $[M+Na]^+$: 535.1, found: 535.2.

Synthesis of compound 11[3]

To 40 mL dry MeOH was added **10** (5.12 g, 10 mmol) and sodium methoxide (108 mg, 2 mmol) and stirred at room temperature for 30 min. After completion of the reaction, the mixture was neutralized with Dowex 50WX2 ion-exchange resin, filtered and evaporated to afford **11** (2.37 g, 78.5%) ready for next step. ESI-MS calculated for $C_{13}H_{18}NaO_6S^+$ $[M+Na]^+$: 325.1, found: 325.1.

Synthesis of compound 12

To 60 mL dry MeCN was added **11** (950 mg, 3.12 mmol), **8** (400 mg, 1.04 mmol) and Et_3N (14.5 μl, 0.104 mmol) under argon protection. The mixture was stirred at room temperature for 48 h. Then, the solution was diluted with MeOH and purified by silica gel column (DCM: MeOH = 15: 1) to afford **12** (358 mg, 49.2%). ^{1}H NMR (400 MHz, $CDCl_3$) δ 8.94 (s, 1H), 7.39 (m, 3H), 7.20 (m, 2H), 6.83 (d, J = 8.1 Hz, 2H), 6.76 (d, J = 8.1 Hz, 2H), 6.45 (s, 1H), 4.73 (m, 1H), 4.48 (m, 1H), 4.38 (m, 1H), 4.20 (m, 1H), 4.00 (m, 2H), 3.62 (m, 2H), 3.40 (m, 1H), 2.67 (s, 3H), 2.32 (q, J = 7.4 Hz, 2H), 1.39 (s, 3H), 0.97 (t, J = 7.4 Hz, 3H). ESI-MS calculated for $C_{33}H_{36}BF_2N_2O_7S^+$ $[M+H]^+$: 653.2, found: 653.3.

Synthesis of compound BOD-L-*β*Gal

Compound **12** (300mg, 0.46 mmol) was dissolved in freshly distilled EtOH (20 mL), followed by the addition of malononitrile (92 mg, 1.38 mmol). The solution was stirred for 5 h at 90 °C under argon. After cooling to room temperature, the solvent was removed *in vacuo* and the residue was purified by silica gel column (DCM: MeOH = 15: 1) to afford **BOD-L-*β*Gal** (150mg, 46.5%). ^{1}H NMR (400 MHz, DMSO-d_6) δ 7.65 – 7.41 (m, 6H), 7.02 (d, J = 8.3 Hz, 2H), 6.92 (d, J = 8.0 Hz, 2H), 6.81 (s, 1H), 5.15 (m, 1H), 4.91 (m, 1H), 4.76 (m, 1H), 4.64 (m, 1H), 4.53 (m, 1H), 4.11 (m, 2H), 3.52 (m, 4H), 2.73 (s, 3H), 2.43 (q, J =

7.4 Hz, 2H), 1.49 (s, 3H), 1.01 (s, J = 7.4 Hz, 3H). ^{12}C NMR (151 MHz, DMSO-d_6), δ 171.13, 157.31, 151.45, 145.10, 144.28, 140.12, 138.94, 137.05, 136.21, 131.95, 130.27, 130.15, 129.92, 129.68, 128.85, 128.80, 127.10, 118.92, 116.46, 114.51, 113.49, 101.53, 75.44, 73.31, 70.25, 67.95, 62.81, 60.13, 41.25, 40.05, 39.52, 16.57, 14.05, 13.61, 12.37. HRMS (ESI, m/z): calculated for $C_{36}H_{35}BF_2N_4NaO_6S^+$ $[M+Na]^+$: 723.2231, found: 723.2222.

***In vitro* enzymatic assay**

BOD-L-*β*Gal was used at a final concentration of 10 μM. Absorption and fluorescence spectra of **BOD-L-*β*Gal** with *β*-gal enzymatic reactions were performed at 37 °C in a 3 mL total volume of PBS buffer (0.1 M, pH 7.4, 30% DMSO) in a 1 cm cuvette. UV–vis absorption spectra were recorded on U-2900 Spectrophotometer (Hitachi, Japan). Fluorescence spectra were measured with F-7000 Fluorescence Spectrophotometer (Hitachi, Japan).

Preparation of PLGA Nanoparticles

Poly(lactic-co-glycolic acid) (PLGA) polymer with an average molecular weight of 20,000 and a lactide-to-glycolide copolymer ratio of 75:25 (Jinan Daigang Biomaterial Co., China) was used to prepare the nanoparticles. PLGA nanoparticles incorporated with **BOD-L-*β*Gal** were prepared by a previously reported emulsion solvent diffusion method in purified water[4-7]. PLGA (100 mg) was dissolved completely in 2 mL acetone and 1 mL methanol. Then, **BOD-L-*β*Gal** was added to this solution. The resultant organic solution was emulsified into 25 mL of an aqueous PVA solution (1.0%, w/v) and stirred at 400 rpm using a propeller-type agitator with 3 blades for 30 min. After the mixture was agitated for 2 h under reduced pressure at 40 °C, the entire dispersed system was then centrifuged (43,400 × g for 10 min at -20 °C, Hitachi CP-100NX, Japan), resuspended in distilled water and centrifuged again to remove excess polyvinyl alcohol and the unencapsulated reagent that could not absorb onto the surfaces of the nanoparticles. After the process was repeated, the resultant dispersion was dried using a freeze drying method. The encapsulation efficiency (EE) and loading capacity (LC) of **BOD-L-*β*Gal-NPs** were qualified by a HPLC system (Agilent 1200, USA) after the samples were demulsified by acetone. The EE and LC of **BOD-L-*β*Gal** in **BOD-L-*β*Gal-NPs** were approximately $55.78 \pm 4.88\%$ and $9.69 \pm 0.84\%$

(w/w), respectively. The average diameters of the **BOD-L-*β*Gal-NPs** were 152.3 ± 6.5 nm , the PdI is 0.123 and the surface charges (zeta potential) analyzed by Zetasizer Nano (Malvern ZEN 3600 Zetasizer Nano System) were -18.7 ± 0.3 mV.

Cell experiment

The culture of primary rat vascular smooth muscle cells (VSMCs)

VSMCs were isolated from the aortic arteries of rats as reported previously[8-9]. Male Sprague Dawley (SD), 80-100g, were anesthetized with sodium pentobarbital (40 mg/kg, Sigma). The isolated VSMCs were cultured in Dulbecco's modified Eagle's medium (DMEM, HyClone) supplemented with 10% fetal bovine serum (FBS, Gibco), 1% penicillin-streptomycin (Gibco), and were used at bioimaging.

***In vitro* cytotoxicity assay**

The cytotoxicity of **BOD-L-*β*Gal** and **BOD-L-*β*Gal-NPs** towards VSMCs was measured by the cell counting kit-8 (CCK-8 kit, Beyotime Biotechnology, Jiangsu, China). Briefly, VSMCs were plated in 96 well plates at a density of 5,000 cells/well in 0.1 mL volume of serum-free culture media. The following day, cells were treated with desired concentrations of **BOD-L-*β*Gal** or **BOD-L-*β*Gal-NPs**. After incubation for 24 h, 10 μl CCK-8 solution was added to each well, then, the absorbance was measured at 450 nm with a microplate reader (Varioskan Flash Multimode Reader, Thermo Scientific, USA). Data were collected in three independent experiments.

Fluorescence imaging under the senescent condition

For fluorescence imaging, the senescent condition was initially induced by the treatment of Ang II (Merck) consistent with a previously reported method[4,10]. Briefly, VSMCs were plated in Glass Bottom Cell Culture Dish (NEST) at a density of 8×10^4 cells/mL. After cultures reached confluence in growth medium, VSMCs were transferred to serum-free medium and incubated with Ang II at 5 μM for 3 days. Since Ang II, a peptide drug, is easily degraded, the growth medium should be refreshed every 12 h. VSMCs untreated with Ang II cultured with serum-free medium and cells cultured with serum-containing medium were used as controls. After 3 days, all cells were washed and incubated in serum-free medium containing 10 μM of **BOD-L-*β*Gal** for 1 h. Live cell images were acquired using Carl Zeiss LSM710

with a 20 × objective. Green fluorescence was excited at 488 nm and emission was collected at 569-623 nm. Red fluorescence was excited at 561 nm and emission was collected at 698-754 nm.

Fluorescent staining of VSMCs with Hoechst 33258

Hoechst 33258 is a kind of fluorescent dye which is sensitive to DNA conformation and chromatin state in cells[11-12]. Apoptosis is characterized by specific structural changes that include nuclei-shrunk and nuclear condensation[11-12]. Therefore, Hoechst 33258 could be used to detect the degree of nuclear damage. After staining with **BOD-L-*β*Gal**, cells were washed with PBS, fixed with 4% paraformaldehyde for 10 min at room temperature, washed twice with PBS and then stained with Hoechst 33258 for 10 min at room temperature. After three washed with PBS, Live cell images were acquired using Carl Zeiss LSM710 with a 20× objective. Blue fluorescence was excited at 405 nm and emission was collected at 410-495 nm. Green fluorescence was excited at 488 nm and emission was collected at 569-623 nm. Red fluorescence was excited at 561 nm and emission was collected at 698-754 nm.

Experimental Animals

The animal experiments were reviewed and approved by our institutional review board. Male ApoE$^{-/-}$ mice (C57BL/6 background) were obtained from National Resource Center of Model Mice (China). Animals were maintained under a 12-hour light/dark cycle with free access to normal rodent chow and water. Mice (4 to 6 months old) were anesthetized by isoflurane, and an osmotic minipump (Alzet model 2004, Durect Corp, Calif) was implanted to deliver Ang II subcutaneously at a dose of 1.44 mg $\cdot kg^{-1} \cdot d^{-1}$ for 4 weeks.

Animals experimental protocol

At 12 weeks of age, mice began receiving the high-fat diet (Research Diets, USA). After 4 weeks of high-fat diet, all mice were infused with angiotensin II dissolved in PBS at 1.44 mg $\cdot kg^{-1} \cdot d^{-1}$ via an osmotic mini-pump for 4 weeks. Mice were anesthetized with intraperitoneal injection of pentobarbital at day 28 of angiotensin II infusion for imaging. Male C57BL/6 mice, received normal rodent chow and did not treated with angiotensin II, used as control.

Real-time *in vivo* imaging in senescent mice

At day 28 of angiotensin II infusion, *in vivo* fluorescence imaging in angiotensin II-infused mice was performed at 24 h, following intravenous injection of **BOD-L-*β*Gal** (300 μL, 3.3 mg/mL) or **BOD-L-*β*Gal-NPs** (300 μL, 33.3 mg/mL), using an *in vivo* fluorescence imaging system (VISQUE InVivo Smart, Republic of Korea) by Cy5.5 model (Ex: 630-680 nm, Em: 690-740 nm). Whole-body images were obtained from an anesthetized epilatory mouse and analyzed with CleVue software.

***Ex vivo* imaging of different sections of fresh organs after BOD-L-*β*Gal or BOD-L-*β*Gal-NPs treatment**

For *ex vivo* imaging, mice, following intravenous injection of **BOD-L-*β*Gal** (300 μL, 3.3 mg/mL) or **BOD-L-*β*Gal-NPs** (300 μL, 33.3 mg/mL), were euthanized with intraperitoneal injection of pentobarbital, and organs were analyzed immediately after harvesting. Fluorescence images were taken on VISQUE InVivo Smart by using Cy5.5 model (Ex: 630-680 nm, Em: 690-740 nm).

Histology

To detect *β*-Gal activity in senescent VSMCs and examine cellular senescence in the aorta, X-gal staining was conducted using a commercially available Senescence Cells Histochemical Staining Kit (sigma, USA), according manufacture's instructions. Images of senescent VSMCs by X-gal staining were acquired using Inverted Microscope (Leica DMI4000 B, UK). Images of senescent aorta by X-gal staining were acquired using Stereo Microscope (Olympus, SZX16, Japan). To evaluate the extent of atherosclerosis, the aortic arch and the thoracic aorta was opened longitudinally, stained with Oil Red O, and pinned on a black wax surface. Images of Oil Red O staining were acquired using (Olympus, SZX16, Japan).

Western blot analysis

Samples were prepared in radioimmunoprecipitation assay (RIPA) lysis buffer (Thermo Fisher, USA) with 1X protease and phosphatase inhibitor cocktail (Selleck Chemicals). The lysates were centrifuged at 12,000 rpm for 15 min at 4 ^{o}C. The supernatant was extracted and protein content was determined by Protein Quantitation Kit (Invitrogen, USA). 30 μg of total protein was subjected to sodium dodecyl sulfate polyacrylamide gel electrophoresis (SDS-PAGE). Proteins were transferred to a polyvinylidine difluoride

membranes (Millipore, USA) and blocked with 5% bovine serum albumin (BSA) for 1 h at room temperature. Primary antibodies were incubated on the membranes for *β*-Gal (Cell Signaling Technology, USA), MMP9 (Proteintech, USA) and GAPDH (Proteintech, USA) overnight at 4 ^{o}C. The membranes were then incubated for 1 h at room temperature with a horseradish peroxidase-conjugated secondary antibodies (Cell Signaling Technology, USA). Immunoreactive straps were identified using the enhanced chemilumi-nescence (ECL) system (Millipore, USA) according to the manufacturer's protocol. The Bio-Rad system imager was used to visualize the specific bands, and the optical density of each band was measured using the Image J software (NIH, Bethesda, MD, USA). The ratio between integrated optical density (IOD) of the target proteins and GAPDH of the same sample was calculated as relative content and expressed graphically.

Results and Discussion

Table S1 Enzyme kinetics parameters of **BOD-L-*β*Gal** and reported *β*-gal probes.

substrate	Km(μM)	Vm(μM · S^{-1})	Ref
BOD-L-*β*Gal	34.60	13.52	This work
DCM-*β*gal	60.1	0.54	[13]
SG1	1.73	0.0163	[14]
FDG	10.2	0.00033	[14]
X-gal	260.58	0.04	[13]

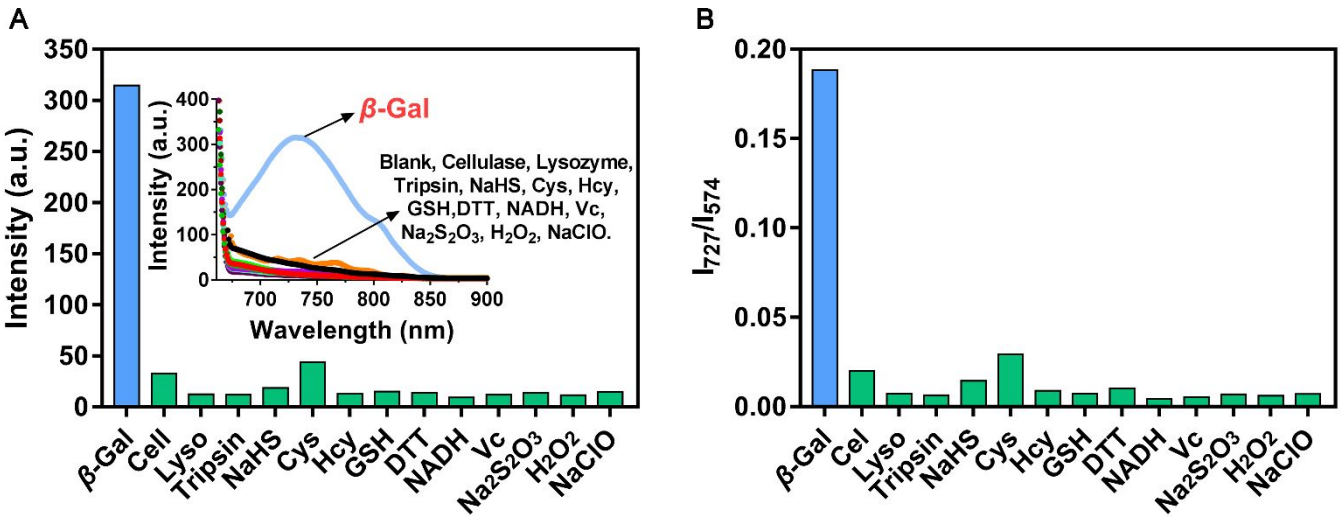

Figure S1 The selectivity of BOD-L-*β*Gal for *β*-Gal. (A) Fluorescence responses of BOD-L-*β*Gal (10 μM) to various analytes in an aqueous system (PBS/DMSO = 7:3 v:v; pH = 7.4, 37 °C) with *β*-Gal (14 U), cellulose (1 kU), lysozyme (1 kU), trypsin (1 kU), NaHS (1 mM), Cys (1 mM), Hcy (1 mM), GSH (1 mM), DTT (1 mM), NADH (1 mM), Vc (1 mM), $Na_2S_2O_3$ (1 mM), H_2O_2 (1 mM), and NaClO (1 mM). λ_{ex} = 651 nm. The inset shows the fluorescence spectra of BOD-L-*β*Gal upon reacting with different kinds of species. λ_{ex} = 651 nm. (B) Fluorescence ratio (I_{727} nm/I_{574} nm) responses of BOD-L-*β*Gal (10 μM) to various analytes in an aqueous system (PBS/DMSO = 7:3 v:v; pH = 7.4, 37 °C) with *β*-Gal (14 U), cellulose (1 kU), lysozyme (1 kU), trypsin (1 kU), NaHS (1 mM), Cys (1 mM), Hcy (1 mM), GSH (1 mM), DTT (1 mM), NADH (1 mM), Vc (1 mM), $Na_2S_2O_3$ (1 mM), H_2O_2 (1 mM), and NaClO (1 mM). For I_{727} nm, λ_{ex} = 651 nm; and for I_{574} nm, λ_{ex} = 488 nm. The inset shows the fluorescence spectra of BOD-L-*β*Gal upon reacting with different kinds of species. λ_{ex} = 651 nm.

Elemental Composition Report **Page 1**

Single Mass Analysis
Tolerance = 10.0 PPM / DBE: min = -1.5, max = 50.0
Element prediction: Off
Number of isotope peaks used for i-FIT = 2

Monoisotopic Mass, Even Electron Ions
25 formula(e) evaluated with 1 results within limits (up to 50 closest results for each mass)
Elements Used:
C: 0-23 H: 0-20 N: 0-5 S: 1-1 B: 0-1 F: 0-2

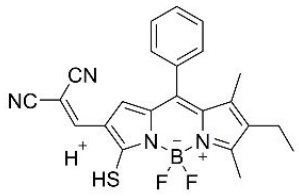

Chemical Formula: $C_{23}H_{20}BF_2N_4S^+$
Exact Mass: 433.1464

CC-ZHAO
ZC-WRC-001 50 (0.564) Cm (50:52)

1: TOF MS ES+
1.53e+003

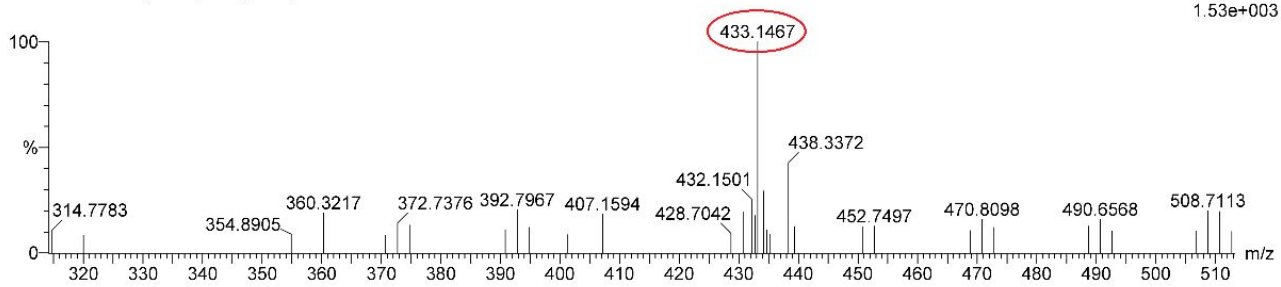

Minimum:				-1.5			
Maximum:		5.0	10.0	50.0			
Mass	Calc. Mass	mDa	PPM	DBE	i-FIT	i-FIT (Norm)	Formula
433.1467	433.1470	-0.3	-0.7	15.5	20.1	0.0	C23 H20 N4 S B F2

Figure S2 ESI-MS spectra characterization of **BOD-L-*β*Gal** reaction with *β*-gal.

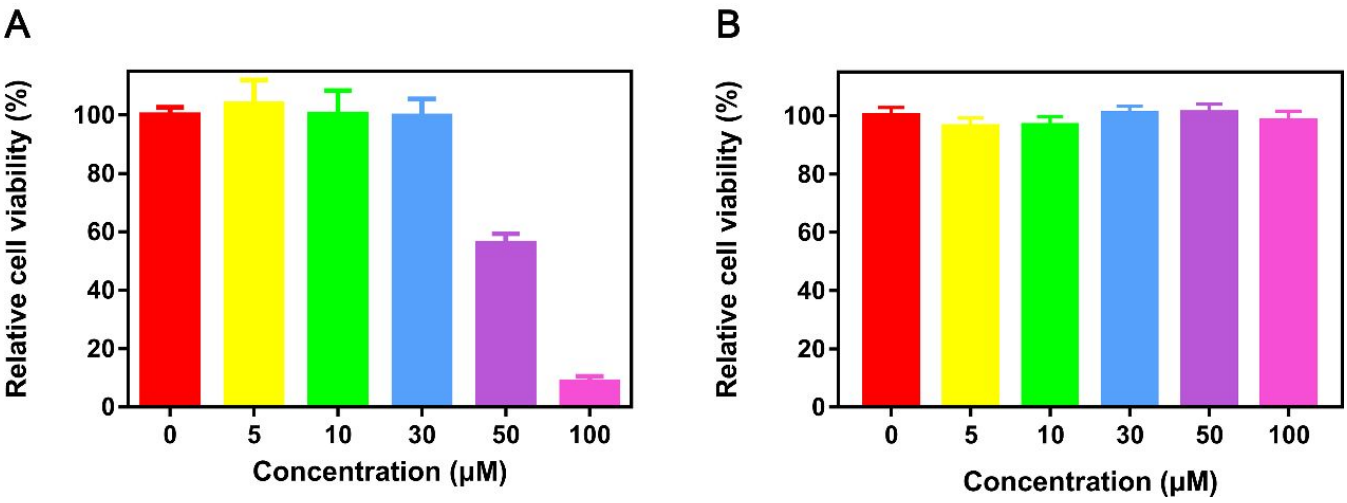

Figure S3. Relative *vitro* viability of primary VSMCs after incubation for 24 h with (A) **BOD-L-*β*Gal** and (B) **BOD-L-*β*Gal-NPs** at various concentrations. Note: **BOD-L-*β*Gal-NPs** have less toxicity and superior biocompatibility toward primary VSMCs to **BOD-L-*β*Gal**.

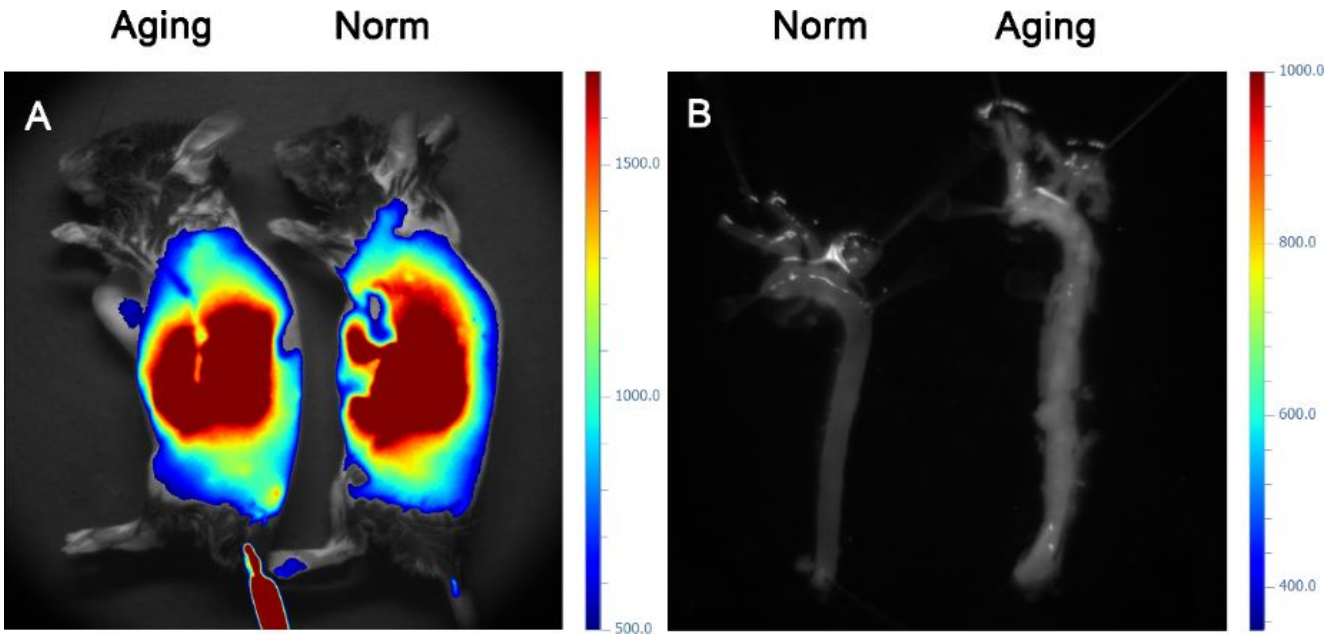

Figure S4 Fluorescence imaging of the Ang II-treated mouse and the control after injecting **BOD-L-*β*Gal** (300 μl, 3.33 mg/ml) via intravenous injection for 1 day (A). Fluorescence images of aortic arch of the Ang II-treated mouse and the control after anatomy following injecting **BOD-L-*β*Gal** for 1 day (B).

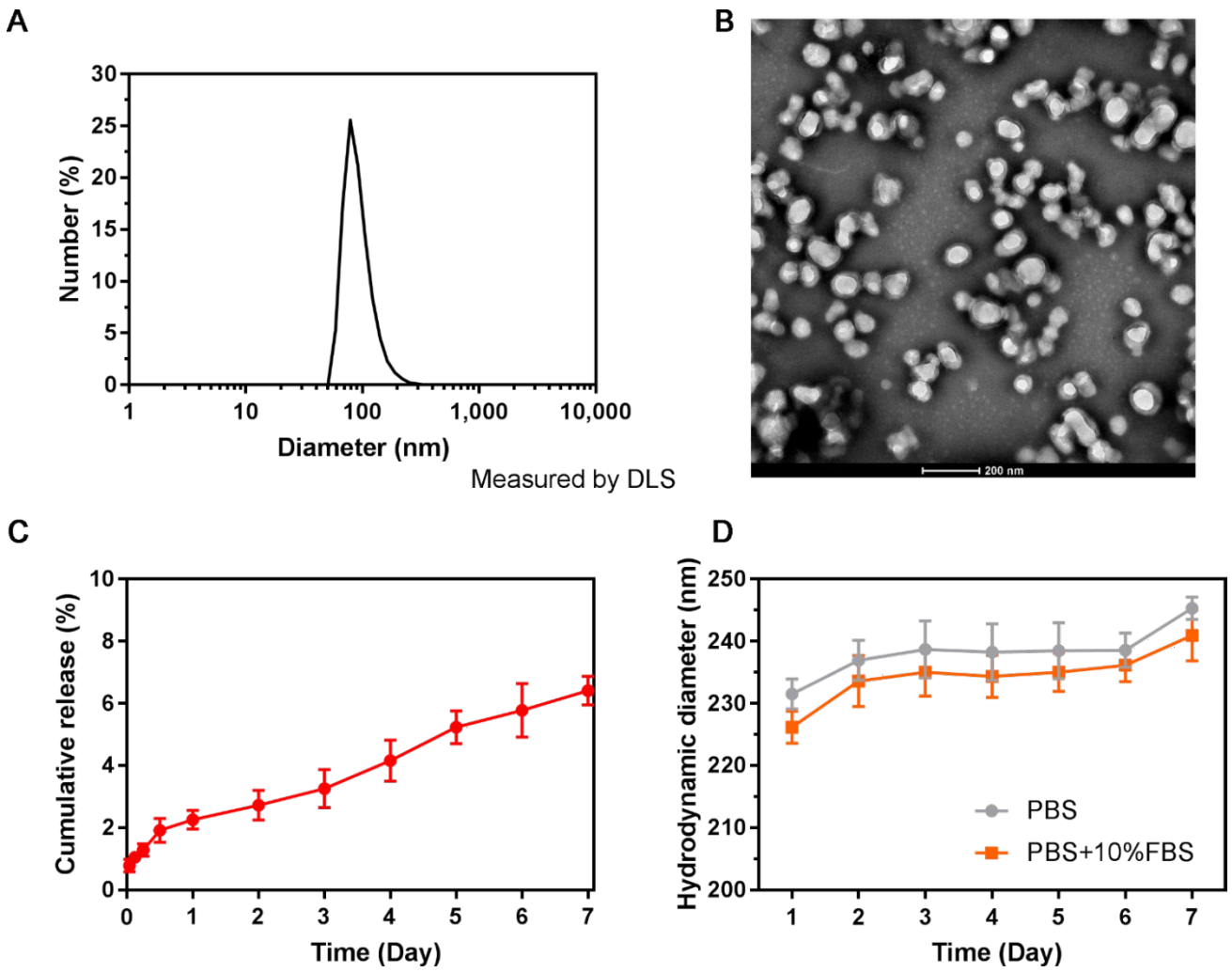

Figure S5 Hydrodynamic diameters of **BOD-L-*β*Gal-NPs** measured by DLS (A). TEM image of **BOD-L-*β*Gal-NPs** (B). Release profile of **BOD-L-*β*Gal** from **BOD-L-*β*Gal-NPs** in PBS (C). Stability of **BOD-L-*β*Gal-NPs** kept in 4 °C conditions monitored by dynamic light scattering (D). Error bars represent S.D. The experiments were performed three times.

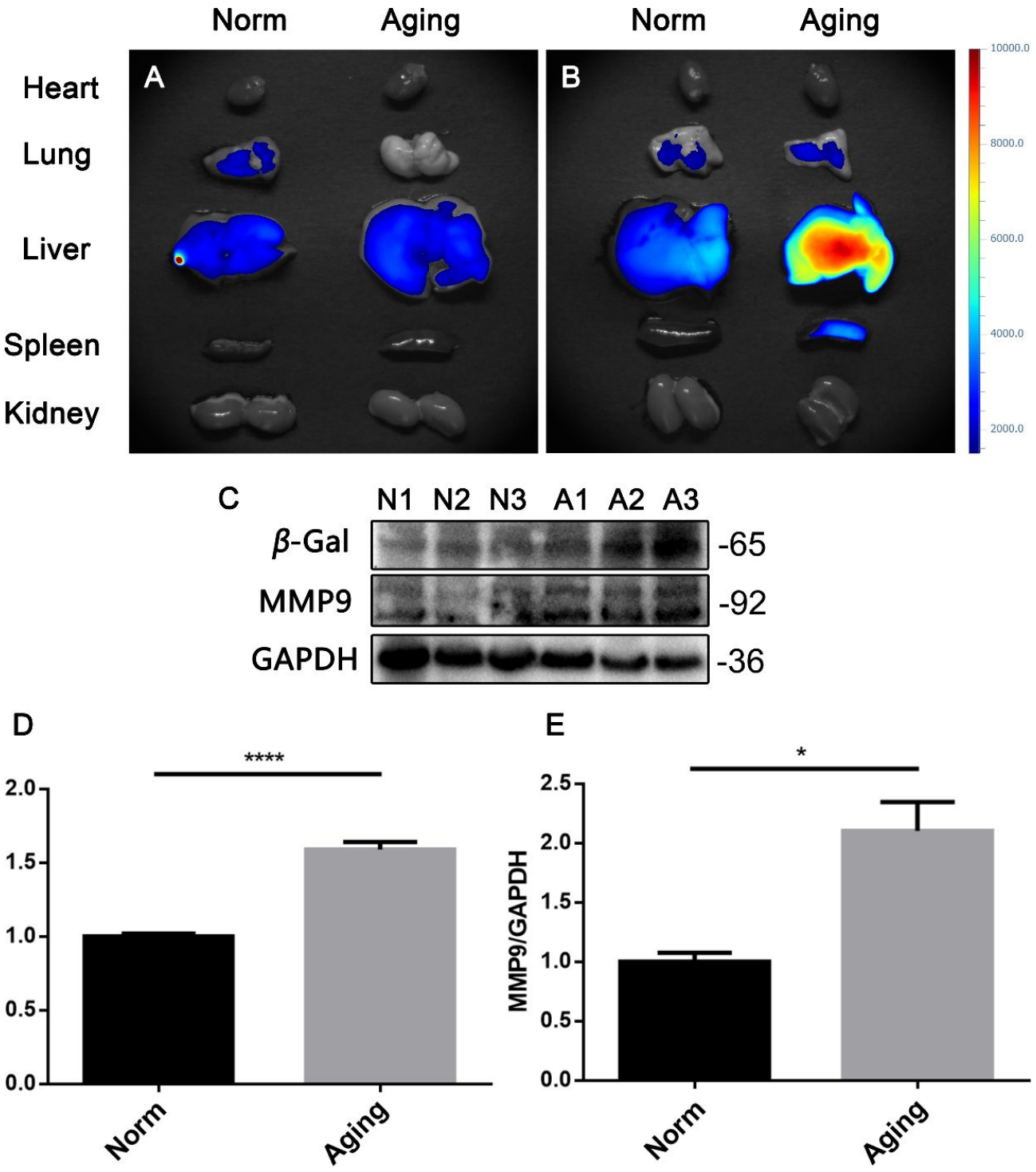

Figure S6 Fluorescence imaging of the main internal organs after anatomy following injection of **BOD-L-*β*Gal** (300 μl, 3.3 mg/mL) via intravenous injection for 1 day (A) or injecting **BOD-L-*β*Gal-NPs** (300 μl, 33.3 mg/ml) via intravenous injection for 1 day (B). Western blotting analysis showed that Ang II significantly up-regulated the expression of senescent associated protein *β*-Gal and MMP9 in liver of 3 Ang II-treated mice (A1-A3) to those of control (N1-N3) (C). Values were normalized to control (1.0)

(D, E). Error bars represent S.D. The experiments were performed three times: (∗) $p < 0.05$, (∗∗) $p < 0.01$, (∗∗∗) $p < 0.001$, (∗∗∗∗) $p < 0.0001$ compared to control.

Figure S7 Bright images of aortic arch of the Ang II-treated mouse and the control acquired using Stereo Microscope (Olympus, SZX16, Japan).

Figure S8 Bright images of aortic arch of the Ang II-treated mouse and the control after Red Oil O staining acquired using Stereo Microscope (Olympus, SZX16, Japan).

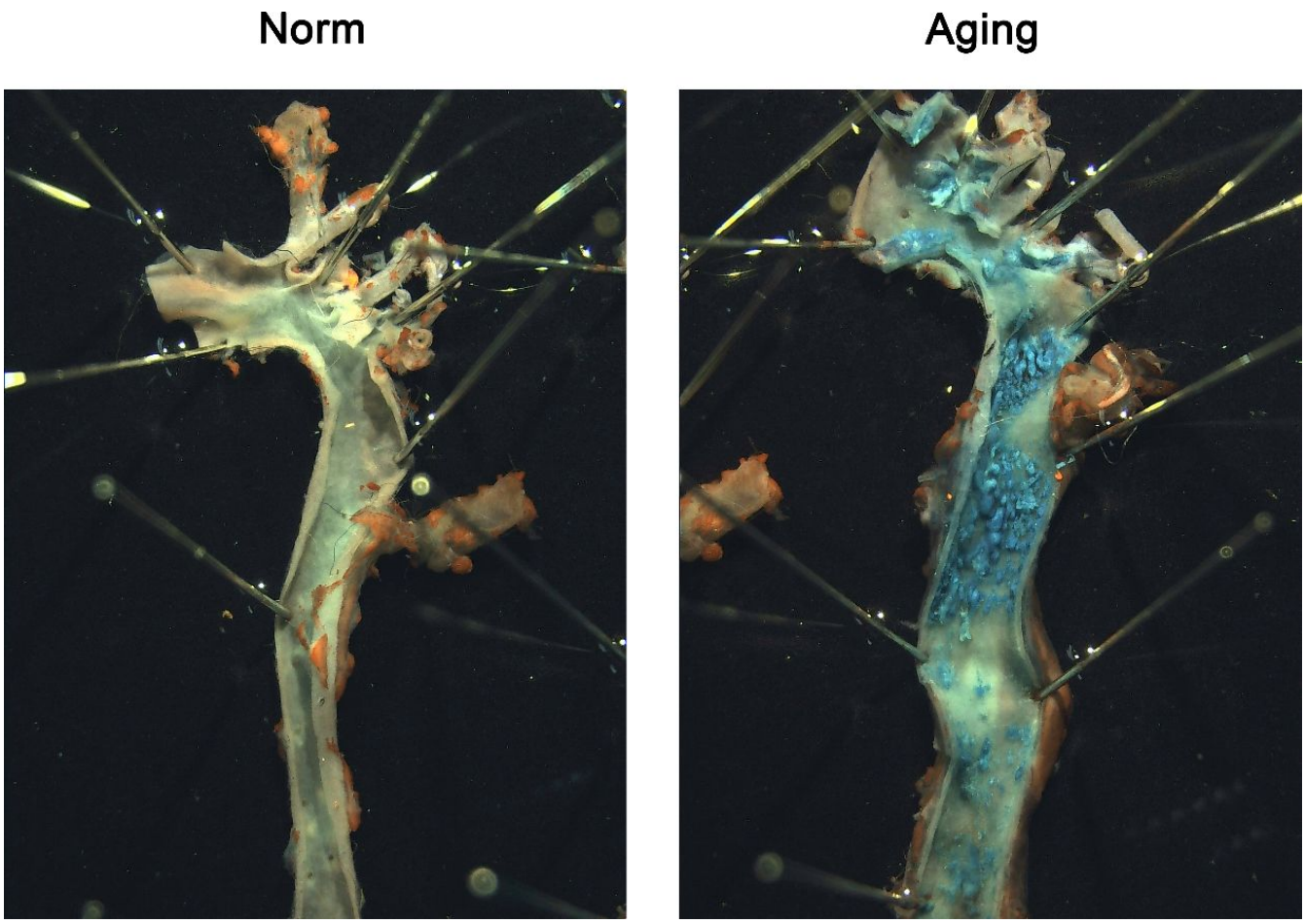

Figure S9 Bright images of aortic arch of the Ang II-treated mouse and the control after whole-mount S-A-*β*-Gal staining acquired using Stereo Microscope (Olympus, SZX16, Japan).

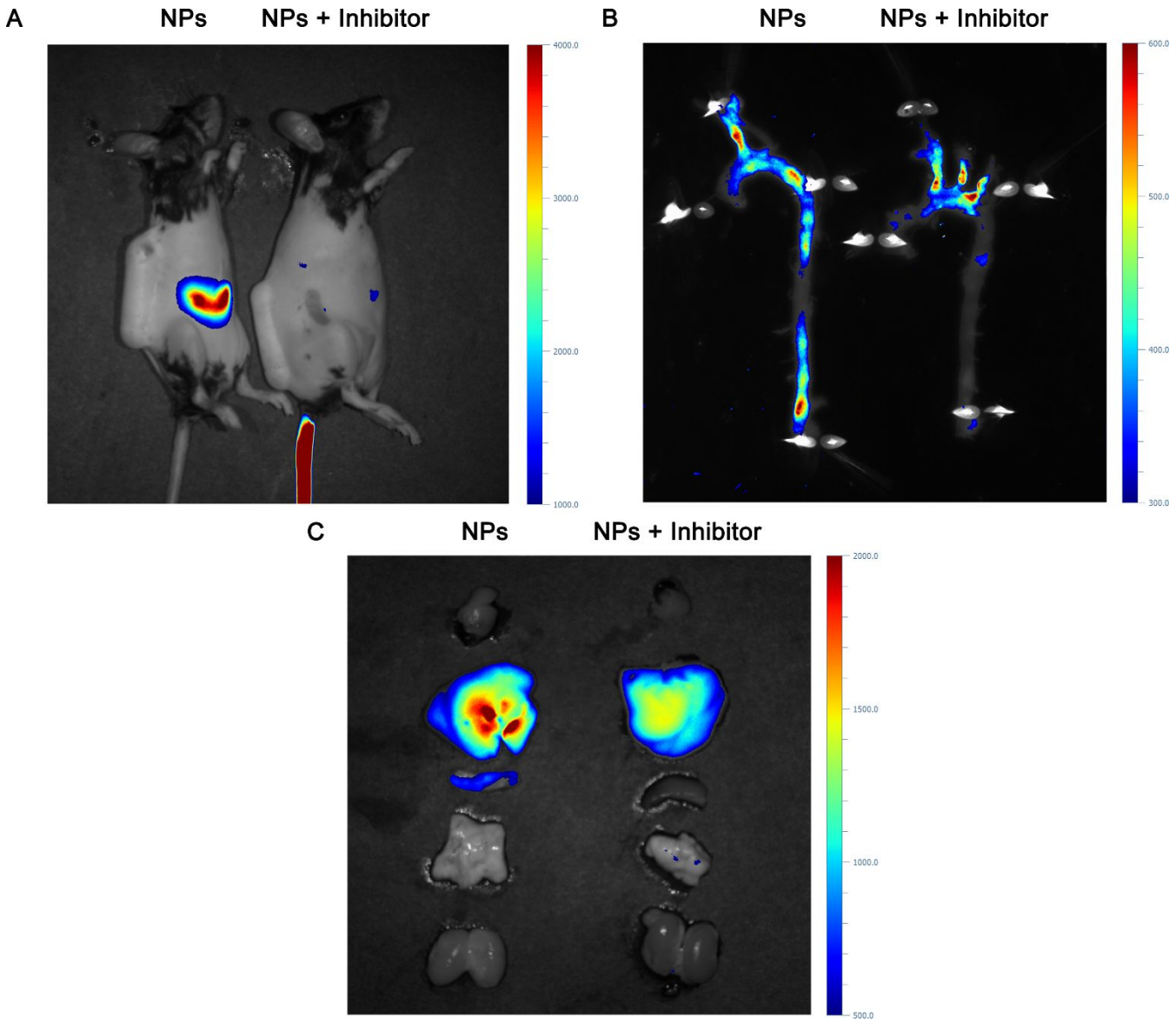

Figure S10 (A) Fluorescence imaging of atherosclerotic mice treated with **BOD-L-*β*Gal-NPs** and Inhibitor-NPs via intravenous injection for 1 day. (B) Fluorescence images of aortic arch of the Ang II-treated mouse after the injection of **BOD-L-*β*Gal-NPs** and Inhibitor-NPs via intravenous injection for 1 day. (C) Fluorescence imaging of the main internal organs after anatomy following injection of **BOD-L-*β*Gal-NPs** and Inhibitor-NPs via intravenous injection for 1 day.

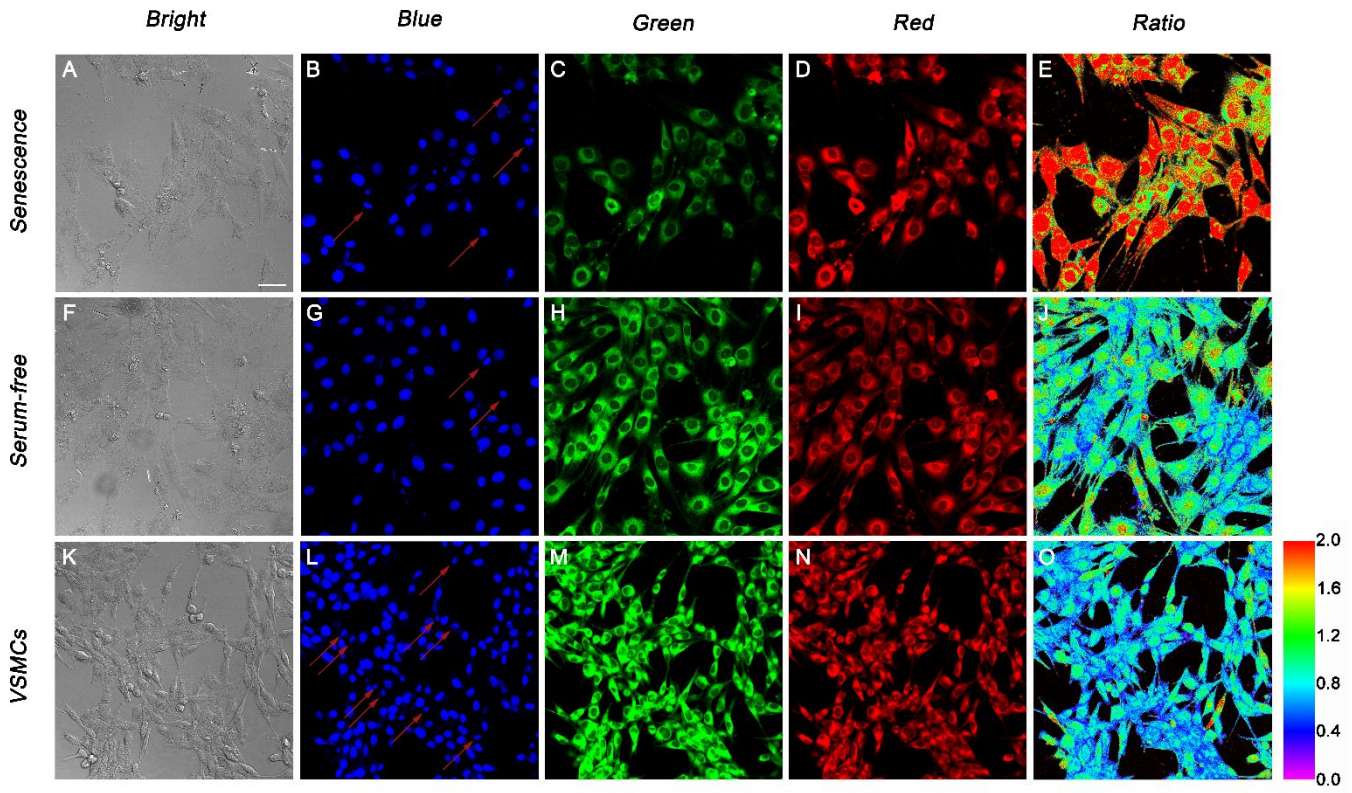

Figure S11 The imaging of Ang II-treated VSMCs (A-D), serum-free-treated VSMCs (F-I) and primary VSMCs (K-N) using **BOD-L-*β*Gal** (10 μM) for 1 h (3^{th}-4^{th} column) and Hoechst 33258 (2^{rd} column). The blue channel was obtained from 410 to 495 nm (λ_{ex} = 405 nm), The green channel was obtained from 550 to 580 nm (λ_{ex} = 488 nm), and the red channel was obtained from 700 to 740 nm (λ_{ex} = 633 nm). Ratiometric images (5^{th} column) of Ang II-treated VSMCs (E), serum-free-treated VSMCs (J) and primary VSMCs (O) generated from the red channel to green channel. The red arrow marked the cells with nuclei-shrunk or nuclear condensation.

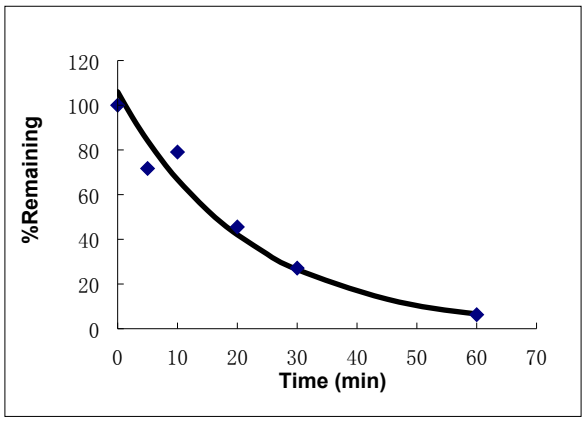

Figure S12 The metabolic stability of **BOD-L-*β*Gal** in human liver microsomes. The $T_{1/2}$ and $C_{lint(liver)}$ of **BOD-L-*β*Gal** were 15.0 min and 83.2 mL/min/mg respectively.

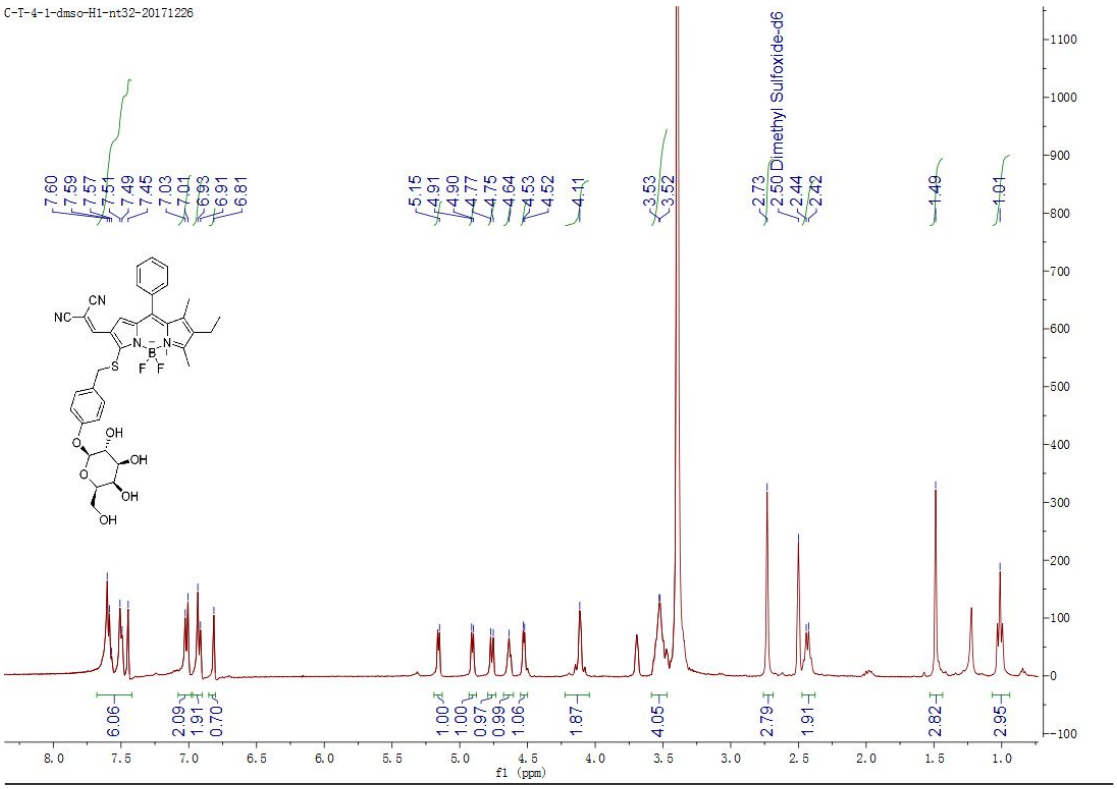

Figure S13 ^{1}H NMR spectrum of **BOD-L-*β*Gal** in DMSO-d_6

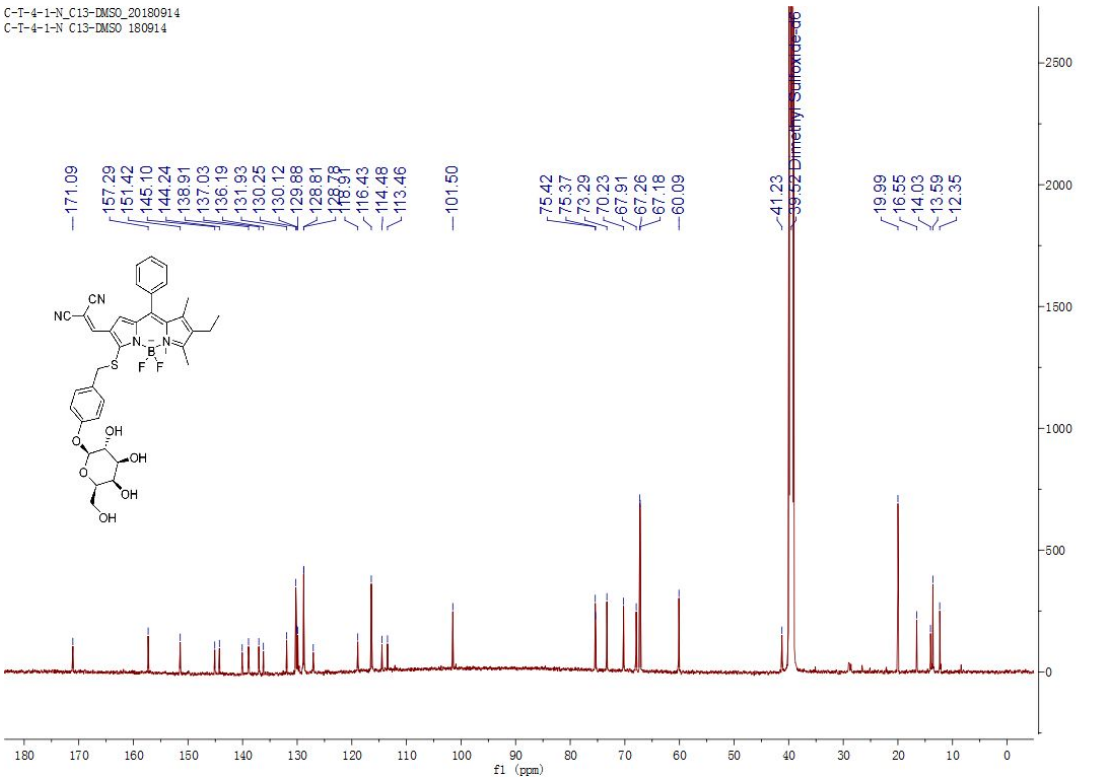

Figure S14 ^{13}C NMR spectrum of **BOD-L-*β*Gal** in DMSO-d_6

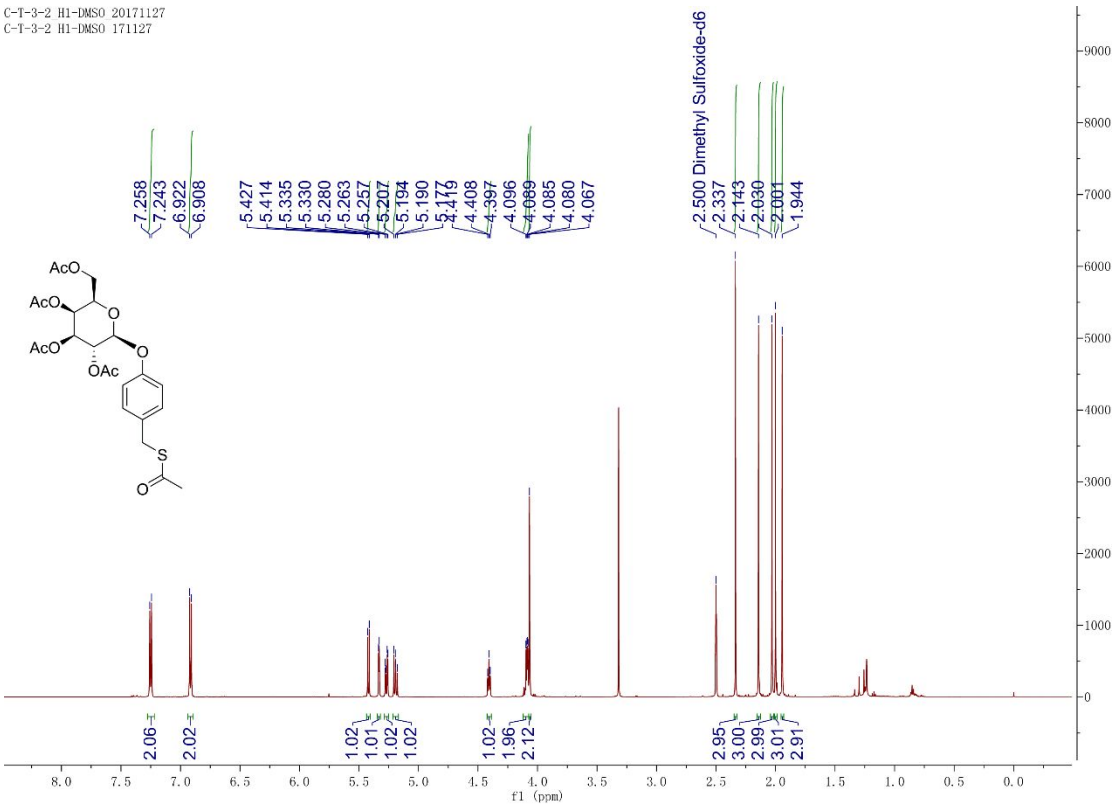

Figure S15 ^{1}H NMR spectrum of **12** in DMSO-d_6

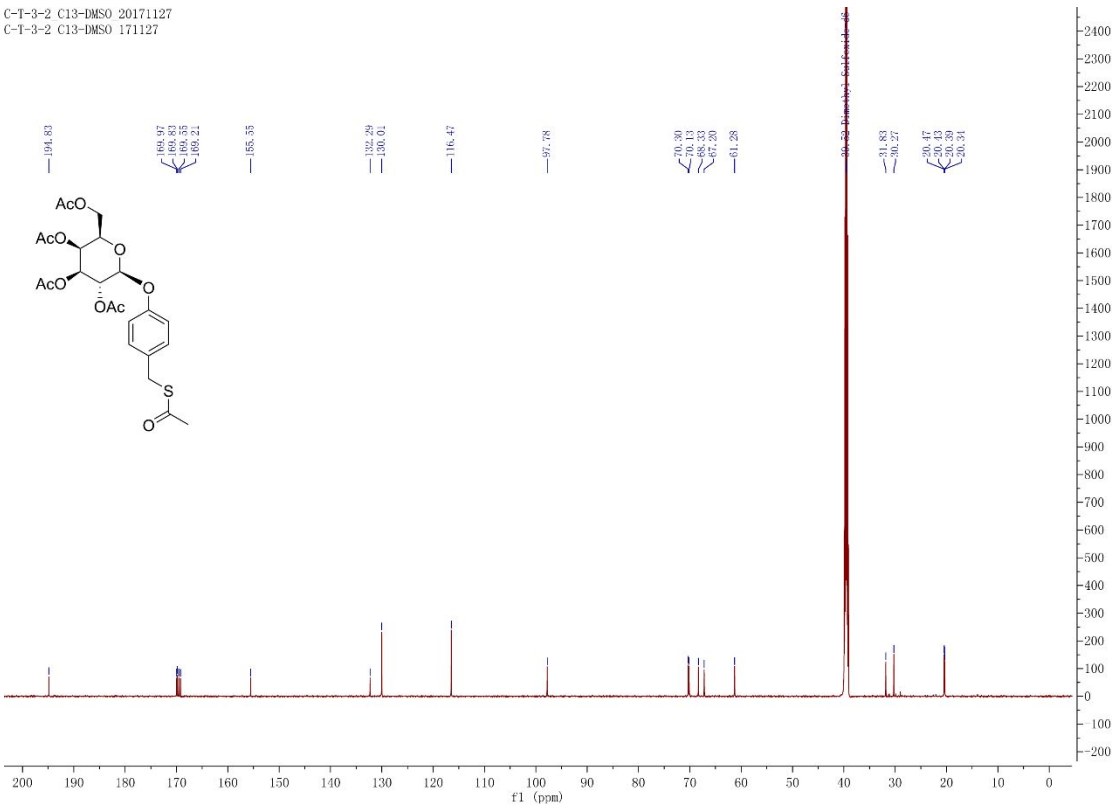

Figure S16 ^{13}C NMR spectrum of **12** in DMSO-d_6

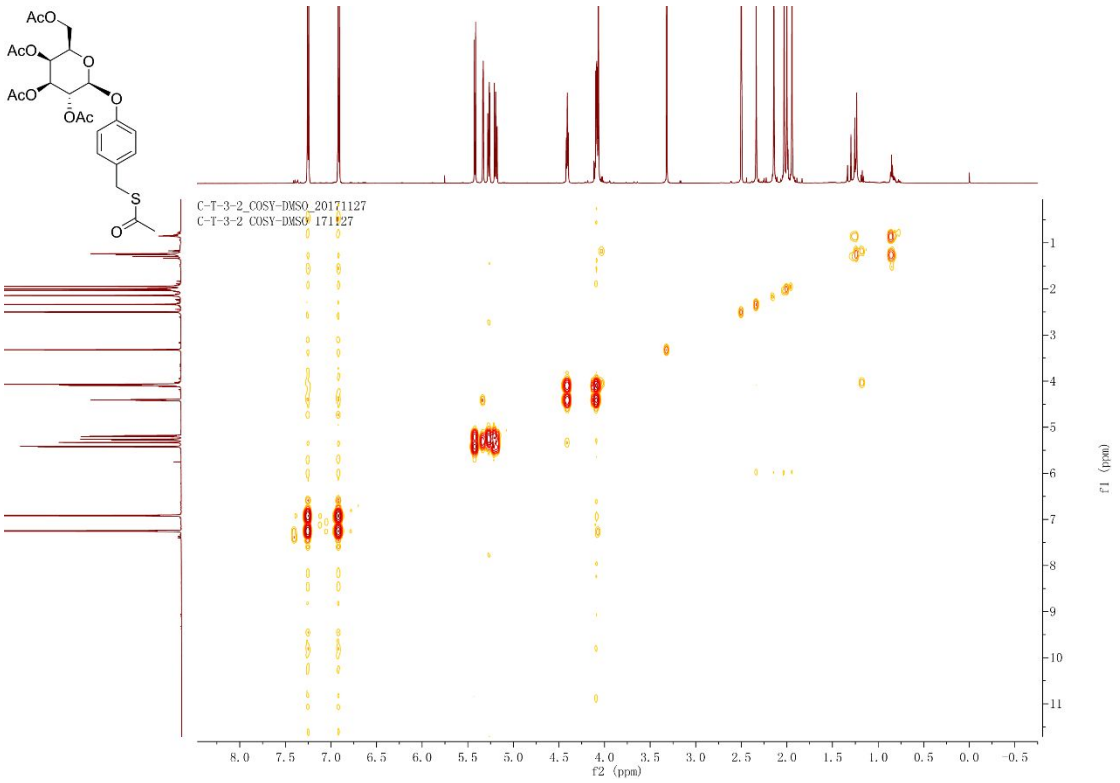

Figure S17 COSY spectrum of **12** in DMSO-d_6

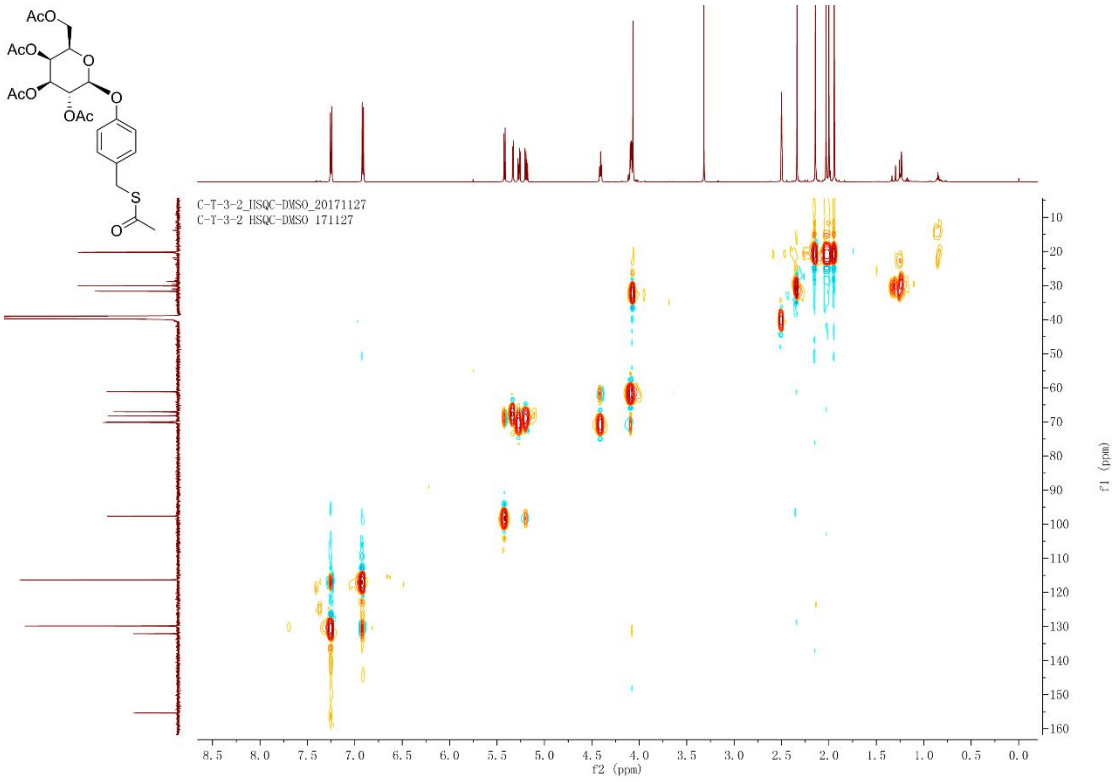

Figure S18 HSQC spectrum of **12** in DMSO-d_6

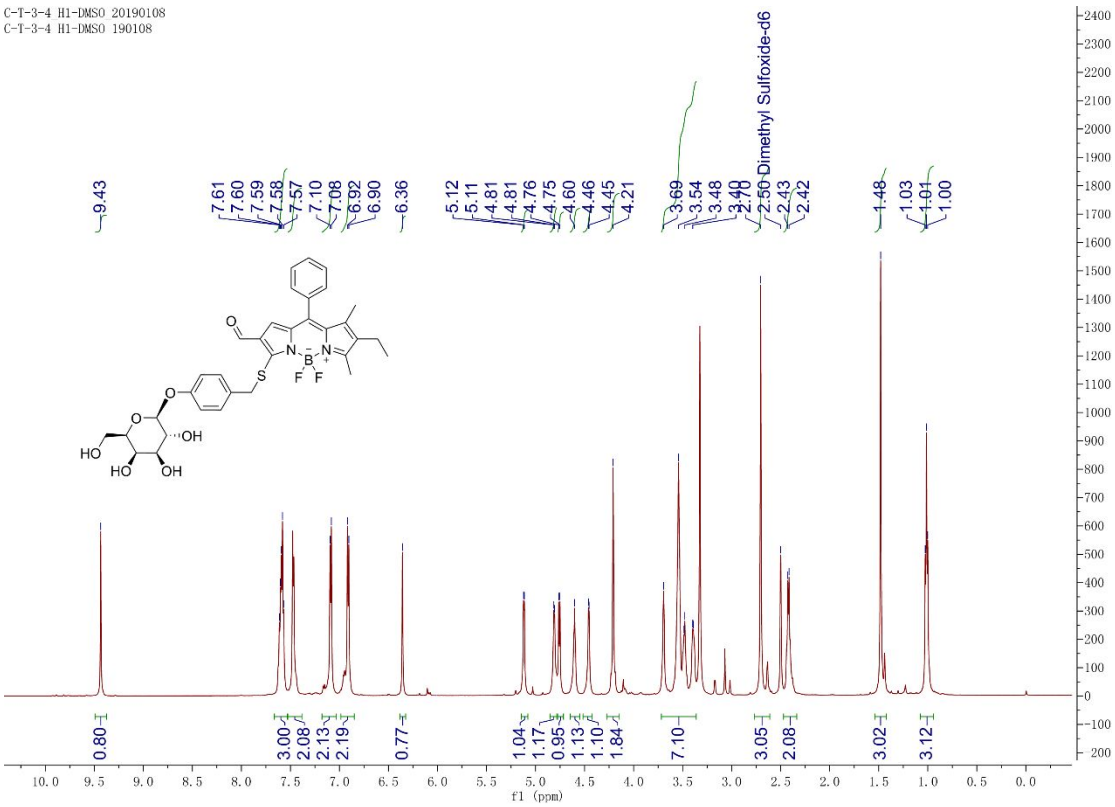

Figure S19 ^{1}H NMR spectrum of **10** in DMSO-d_6

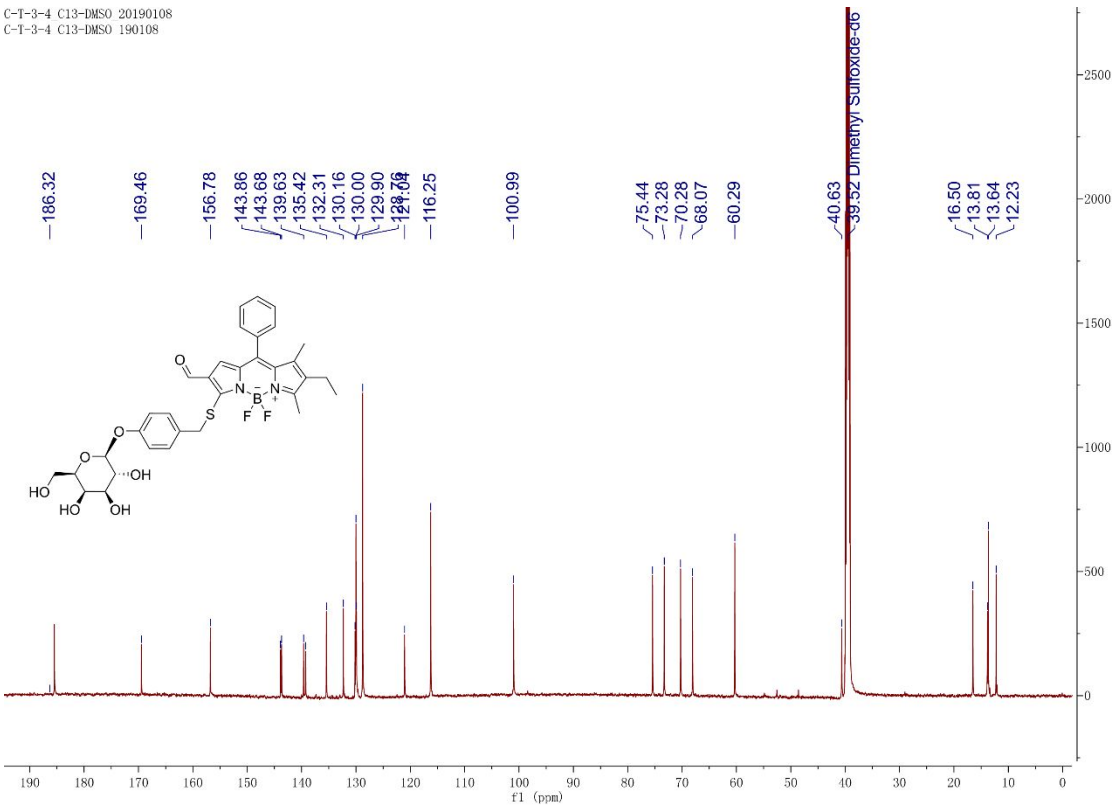

Figure S20 ^{13}C NMR spectrum of **10** in DMSO-d_6

References

[1] Leen V.; Braeken E.; Luckermans K.; Jackers C.; Van der Auweraer M.; Boens N.; Dehaen W. A versatile, modular synthesis of monofunctionalized BODIPY dyes. *Chem. Commun.* **2009**, DOI: 10.1039/b906164a4515.

[2] Mula S.; Ray A. K.; Banerjee M.; Chaudhuri T.; Dasgupta K.; Chattopadhyay S. Design and development of a new pyrromethene dye with improved photostability and lasing efficiency: theoretical rationalization of photophysical and photochemical properties. *J. Org. Chem.* **2008**, *73*, 2146.

[3] Bugaut A.; Jantos K.; Wietor J. L.; Rodriguez R.; Sanders J. K.; Balasubramanian S. Exploring the differential recognition of DNA G-quadruplex targets by small molecules using dynamic combinatorial chemistry. *Angew. Chem. Int. Ed.* **2008**, *47*, 2677.

[4] Katsuki S.; Matoba T.; Nakashiro S.; Sato K.; Koga J.; Nakano K.; Nakano Y.; Egusa S.; Sunagawa K.; Egashira K. Nanoparticle-mediated delivery of pitavastatin inhibits atherosclerotic plaque destabilization/rupture in mice by regulating the recruitment of inflammatory monocytes. *Circulation* **2014**, *129*, 896.

[5] Chen L.; Nakano K.; Kimura S.; Matoba T.; Iwata E.; Miyagawa M.; Tsujimoto H.; Nagaoka K.; Kishimoto J.; Sunagawa K.; Egashira K. Nanoparticle-mediated delivery of pitavastatin into lungs ameliorates the development and induces regression of monocrotaline-induced pulmonary artery hypertension. *Hypertension* **2011**, *57*, 343.

[6] Kawashima Y.; Yamamoto H.; Takeuchi H.; Fujioka S.; Hino T. Pulmonary delivery of insulin with nebulized DL-lactide/glycolide copolymer (PLGA) nanospheres to prolong hypoglycemic effect. *J. Control Release* **1999**, *62*, 279.

[7] Kawashima Y.; Yamamoto H.; Takeuchi H.; Hino T.; Niwa T. Properties of a peptide containing dl-lactide/glycolide copolymer nanospheres prepared by novel emulsion solvent diffusion methods. *Eur. J. of Pharm. Biopharm.* **1998**, *45*, 41.

[8] Luo X.; Yang D.; Wu W.; Long F.; Xiao C.; Qin M.; Law B. Y.; Suguro R.; Xu X.; Qu L.; Liu

X.; Zhu Y. Z. Critical role of histone demethylase Jumonji domain-containing protein 3 in the regulation of neointima formation following vascular injury. *Cardiovasc. Res.* **2018**, *114*, 1894.

[9] Jovinge S.; Hultgårdh-Nilsson A.; Regnström J.; Nilsson J. Tumor Necrosis Factor-α Activates Smooth Muscle Cell Migration in Culture and Is Expressed in the Balloon-Injured Rat Aorta. *Arterioscl. Throm. Vas.* **1997**, *17*, 490.

[10] Kunieda T.; Minamino T.; Nishi J. I.; Tateno K.; Oyama T.; Katsuno T.; Miyauchi H.; Orimo M.; Okada S.; Takamura M.; Nagai T.; Kaneko S.; Komuro I. Angiotensin II induces premature senescence of vascular smooth muscle cells and accelerates the development of atherosclerosis via a p21-dependent pathway. *Circulation* **2006**, *114*, 953.

[11] Jia Y.-L.; Dong X.-Y.; Zhou P.-F.; Liu X.-H.; Pan L.-L.; Xin H.; Zhu Y.-Z.; Wang Y. The synthesis and biological evaluation of novel Danshensu-cysteine analog conjugates as cardiovascular-protective agents. *Eur. J. Med. Chem.* **2012**, *55*, 176.

[12] Wang Y.; Cai Y.-P.; Ji J.-S.; Liu Z.-G.; Zhao C.-G.; Zhao Y.-J. Wei T.; Shen X.-Q.; Zhang X.-H.; Li X.-K.; Liang G. Discovery and identification of new non-ATP competitive FGFR1 inhibitors with therapeutic potential on non-small-cell lung cancer. *Cancer Lett.* **2014**, *344*, 82.

[13] Gu K.; Xu Y.; Li H.; Guo Z.; Zhu S.; Zhu S.; Shi P.; James T. D.; Tian H.; Zhu W.-H. Real-Time Tracking and In Vivo Visualization of beta-Galactosidase Activity in Colorectal Tumor with a Ratiometric Near-Infrared Fluorescent Probe. *J. Am. Chem. Soc.* **2016**, *138*, 5334.

[14] Lee H. W.; Heo C. H.; Sen D.; Byun H. O.; Kwak I. H.; Yoon G.; Kim H. M. Y. Ratiometric Two-Photon Fluorescent Probe for Quantitative Detection of beta-Galactosidase Activity in Senescent Cells. *Anal. Chem.* **2014**, *86*, 10001.